Salt Dependence of the Elasticity and Overstretching Transition of Single DNA Molecules

Jay R. Wenner, Mark C. Williams, Ioulia Rouzina, and Victor A. Bloomfield
Department of Biochemistry, Molecular Biology, and Biophysics, University of Minnesota, Saint Paul, Minnesota 55108 USA

ABSTRACT As double-stranded DNA is stretched to its B-form contour length, models of polymer elasticity can describe the dramatic increase in measured force. When the molecule is stretched beyond this contour length, it shows a highly cooperative overstretching transition. We have measured the elasticity and overstretching transition as a function of monovalent salt concentration by stretching single DNA molecules in an optical tweezers apparatus. As the sodium ion concentration was decreased from 1000 to 2.57 mM, the persistence length of DNA increased from 46 to 59 nm, while the elastic stretch modulus remained approximately constant. These results are consistent with the model of Podgornik et al. (2000, J. Chem. Phys. 113:9343-9350) using an effective DNA length per charge of 0.67 nm. As the monovalent salt concentration was decreased over the same range, the overstretching transition force decreased from 68 to 52 pN. This reduction in force is attributed to a decrease in the stability of the DNA double helix with decreasing salt concentration. Although, as was shown previously, the hydrogen bonds holding DNA strands in a helical conformation break as DNA is overstretched, these data indicate that both DNA strands remain close together during the transition.

INTRODUCTION

Parameters characterizing the flexibility and elasticity of DNA can be obtained by stretching single molecules of DNA. (Cluzel et al. 1996; Rief et al. 1999; Smith et al. 1996) These experiments move one end of a DNA molecule while measuring force at the opposite end through an optical trap or an atomic force microscopy tip. At low force (F), bends are removed from the DNA and the duplex acts as an entropic spring. This portion of the force–extension curve is well described by the worm-like chain (WLC) model and is dominated by polymer flexibility expressed in terms of persistence length (P_{ds}). (Bustamante et al. 1994; Marko and Siggia 1995; Odijk 1995)

As the end-to-end extension nears the molecular contour length, the force–extension curve begins to rise quickly. At these forces, DNA can be extended slightly beyond its contour length, which is accounted for by the elastic stretch modulus (K_{ds}) parameter in the extensible worm-like chain model (Odijk 1995),

$$b_{ds}(F) = b_{ds}^{max}\left\{1 - \frac{1}{2}\left(\frac{k_B T}{F P_{ds}}\right)^{1/2} + \frac{F}{K_{ds}}\right\}, \qquad (1)$$

where b_{ds} is the extension of the molecule per base pair and b_{ds}^{max} is the dsDNA contour length. Earlier measurements of these parameters as a function of sodium ion concentration ($[Na^+]$) from single molecule stretching (Baumann et al. 1997) cannot be explained by standard elasticity theory, which predicts that P_{ds} and K_{ds} should be proportional. To resolve this inconsistency, a theory describing the elasticity of DNA was proposed (Podgornik et al. 2000) that takes into account the electrostatic repulsion between partially screened phosphate charges on the DNA molecule. It was shown that, while the polyelectrolyte contribution to the persistence length should increase as the solution $[Na^+]$ is lowered, the stretch modulus should decrease with solution $[Na^+]$. The authors fit the data of Baumann et al. (1997) to their theory, which appeared to describe the persistence length measurements, but not the stretch modulus measurements. Here we use a new algorithm for fitting the DNA stretching curves. We explicitly assume the polyelectrolyte nature of $P_{ds}([Na^+])$ and $K_{ds}([Na^+])$ as obtained by Podgornik et al. (2000). By doing so, we fit both dependencies with respect to the single parameter a, which represents the effective length per unit charge on DNA after counterion condensation. This allows us to eliminate one of the three fitting parameters in Eq. 1 and therefore makes the fit more deterministic. We show that this fitting procedure works well and yields a highly reasonable value of $a = 0.67 \pm 0.07$ nm, which agrees with the value of 0.72 nm that follows from counterion condensation theory (Odijk 1977; Skolnick and Fixman 1977; Manning 1978). This new fitting procedure yields a much weaker dependence of K_{ds} on $[Na^+]$ than the one obtained in Baumann et al. (1997).

A second regime in DNA stretching occurs as DNA is extended past its B-form contour length, and the molecule suddenly yields and extends with little additional force. The resulting plateau in the force–extension curve, which signals the cooperative overstretching transition, occurs at ~60–70 pN, and continues until the molecule is stretched to 1.7 times its B-form contour length. At this point, the force again rises rapidly with a slope that depends on stretching

Submitted June 25, 2001, and accepted for publication March 13, 2002.

Address reprint requests to Victor A. Bloomfield, Dept. of Biochemistry, Molecular Biology, and Biophysics, Univ. of Minnesota, 1479 Gortner Ave. Saint Paul, MN 55108. Tel.: 612-625-2268; Fax: 612-625-5780; E-mail: victor.a.bloomfield-1@tc.umn.edu.

Dr. Williams' present address is Dept. of Physics, Northeastern University, 111 Dana Research Center, Boston, MA 02115.

0006-3495/02/06/3160/10 $2.00

rate (Hegner et al. 1999; Clausen-Schaumann et al. 2000). This description only applies to DNA that is allowed to untwist while being stretched. If the DNA is torsionally constrained, more complex curves are obtained that depend upon helical strain (Allemand et al. 1998; Leger et al. 1999).

The molecular origin of the overstretching transition in torsionally relaxed DNA has been attributed to a secondary structure transition from B-form to a stretched or S-form DNA (Cluzel et al. 1996). According to this model, the duplex denatures during the second rise in the force-extension curve at 1.7 times the B-form contour length (Konrad and Bolonick 1996; Lebrun and Lavery 1996; Cizeau and Viovy 1997; Ahsan et al. 1998; Marko 1998; Haijun et al. 1999; Kosikov et al. 1999). Two main ideas supporting the S-form hypothesis are that the DNA does not break when near the end of the overstretch transition, and cross-linked DNA exhibits an overstretch transition somewhat similar to unmodified DNA.

We have shown instead (Rouzina and Bloomfield 2001a, b; Williams et al. 2001a,b) that the overstretching transition represents an equilibrium form of DNA melting, and that the rise in force at 1.7 times the contour length represents nonequilibrium melting that is rate dependent (Hegner et al. 1999; Clausen-Schaumann et al. 2000). According to this picture, DNA does not break near the end of the transition because some bases remain paired or unmelted (Williams et al. 2001a,b). Cross-linked DNA exhibits a similar, but not identical transition because only a fraction of the bases are crosslinked.

Our theoretical framework of force-induced melting has predicted the overstretch force as a function of pH, temperature, and $[Na^+]$ (Rouzina and Bloomfield 2001a,b). We have recently presented experimental results to support the theoretical predictions of the pH and temperature effects on the overstretching transition (Williams et al. 2001a,b). The results presented here show that the overstretching transition force decreases with salt concentration. Based on the observed dependence of the overstretching transition on solution $[Na^+]$, pH, and temperature, we are now able to construct a detailed model of the structure of overstretched DNA. The pH and temperature dependence indicate that the base pairs connecting the DNA strands are broken during the overstretching transition. The salt dependence of the overstretching transition indicates that the two DNA strands remain close together and stretched during the transition. This implies that the majority of the DNA base pairs melt within internal domains rather than from the free ends. This conclusion is consistent with the one-dimensional nature of the DNA melting transition and its sequence heterogeneity. These two factors are known to result in a large number of equilibrium boundaries within DNA throughout its melting transition (Grosberg and Khokhlov 1994; Frank-Kamenetskii et al. 1987).

MATERIALS AND METHODS

The optical tweezers instrument used in this study consists of two counter-propagating 150-mW, 850-nm diode lasers (SDL, San Jose, CA) focused to a spot inside a liquid flow cell with 1.0-N.A. Nikon water-immersion microscope objectives. Force was calibrated by applying a known viscous drag to a trapped bead and evaluating the change in bead position using position-sensitive photodiode detectors (UDT Sensors, Hawthorne, CA). After trapping a bead, the liquid cell surrounding the bead was oscillated at a known frequency and amplitude. The amplitude of the observed oscillating force due to viscous drag on the bead (Mehta et al. 1998) was measured as a function of frequency, giving the detector signal as a function of applied force. The amplitude of this signal was linear in applied force, and this linear relation determined the calibration factor for the two detectors. All measurements were made at room temperature from 20 to 25°C.

To tether single DNA molecules, a 4.4-μm-diameter Streptavidin-coated bead (Bangs Laboratories, Fishers, IN) was trapped in the optical tweezers and transferred by suction to a glass pipette with a 1–2-μm tip. Another bead was captured and held in the optical trap while a dilute solution of DNA, end labeled with biotin, was run through the cell. After tethering one end of the DNA molecule to the trapped bead, the pipette bead was moved to bind the opposite end. The procedure is identical to that described in Fig. 3 of Bennink et al. (1999)

The tethering buffer was 249 mM NaCl and 2 mM Hepes titrated with 1 mM NaOH to obtain pH 7.5 for a $[Na^+]$ of 250 mM. In previous work with Hepes, we found that protonated Hepes does not act as a DNA counterion because its protonated nitrogen is centrally located on a tertiary amine (Wenner and Bloomfield 1999). Other buffers incorporating 2 mM Hepes had $[Na^+] = 0.100$, 0.535, 0.025, and 0.010. The buffer of $[Na^+] = 2.57$ mM used 1 mM Hepes (with 2.07 mM NaCl) and the buffer of $[Na^+] = 1.000$ M used 10 mM Hepes (with 995 mM NaCl). Because DNA bases titrate at pH below 4 or above 10, DNA stretching is insensitive to pH changes around neutrality (Williams et al. 2001a). We have therefore used relatively low buffer concentrations to decrease the uncertainty in buffer $[Na^+]$.

To ensure the cell solution had reached the intended $[Na^+]$, buffer was run through the cell until stretching curves remained constant. For large decreases in $[Na^+]$, two to three cell volumes of lower $[Na^+]$ buffer was run through the cell followed by the target buffer. Tethering in and obtaining at least partial stretching curves in 1 M, and 500, 100, 53.5, 25, and 10 mM buffer verified data in these buffers.

DNA molecules labeled on opposite strands readily break at low $[Na^+]$. DNA that was biotinylated on both ends of the same DNA strand exhibited less breakage, and was labeled as follows. A 69-base oligonucleotide with 12 bases complementary to a 5′ overhang of bacteriophage λ DNA was annealed to one end of the DNA molecule, and a 30-base primer was annealed to the 3′ end of the 69-base oligonucleotide. The DNA was then incubated with biotin-11-dCTP (Sigma, St. Louis, MO), dATP, dTTP, dGTP, and Klenow *exo*$^-$ DNA polymerase (New England Biolabs, Beverly, MA) to incorporate five biotin labels. T4 DNA ligase (New England Biolabs) was added to 16°C to repair single-strand nicks, and the excess nucleotides were removed using Centricon 100 filters. This is the same attachment method used in Williams et al. (2001b), whereas opposite strand attachment was used in Williams et al. (2001a). The resulting measurements of DNA force–extension curves should not depend on the method of attachment of DNA as long as the system is in equilibrium, because, in the absence of macroscopic motion, the force along the entire molecule should be constant.

When a single molecule was tethered between the two beads, force–extension measurements were made by measuring the force on the bead in the trap while moving the pipette a known distance. A schematic diagram of the experiment is shown in Fig. 1. The absolute extension of the molecule was estimated by measuring the distance between the centers of the two beads using an image captured with a CCD camera (Edmund Industrial Optics, Barrington, NJ). The change in position of the pipette

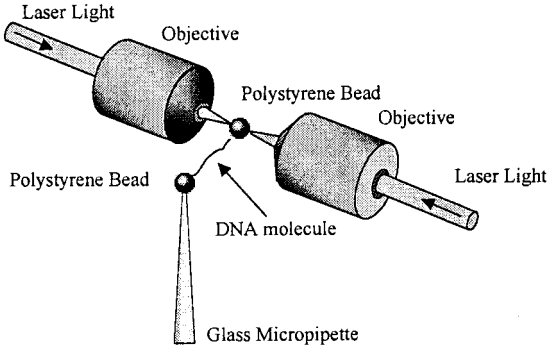

FIGURE 1 Schematic drawing (not to scale) of an optical tweezers experiment in which a single DNA molecule is stretched between two polystyrene beads. One bead is held on the end of a glass micropipette by suction, while another bead is held in an optical trap. Two counter-propagating laser beams focused to a common point form the optical trap.

was measured using a feedback-compensated piezoelectric translation stage that is accurate to 5 nm (Melles Griot, Irvine, CA). The position measurement was converted to a measurement of the molecular extension by correcting for the trap stiffness, which was 60 pN/μm. For the measurements reported here, the pipette was moved in 500-nm steps, and after each step the force was measured 100 times and averaged. Each step took ~0.5 s.

RESULTS

DNA elasticity

Partial stretching curves obtained at salt concentrations ranging from 1000 to 2.57 mM are shown in Fig. 2. All data, with the exception of 2.57 mM, were obtained by tethering and stretching in the same buffer to ensure accurate [Na^+]. Each F versus b curve begins to rise when the B-form contour length of 0.34 nm/bp is approached. Eq. 1 can fit the initial rise in force in the limit of high force ($FP_{ds}/kT > 1$) (Odijk 1995).

Fits of the data to Eq. 1 are shown in Fig. 2. A more accurate model has been proposed (Bouchiat et al. 1999) to replace Eq. 1. However, our measurements at low forces are not accurate enough to distinguish between the models. Because our instrument has a force accuracy of $F = \pm 0.5$ pN, the low force data ($F < 1$ pN; $b_{ds}(F)/b_{ds}^{max} < 0.75$) is not used for the fit. As we will show and as was also discussed in Bouchiat et al. (1999), fitting data over this force regime does not allow a unique determination of the three parameters in Eq. 1. In this force regime, the model of Bouchiat et al. is equivalent to Eq. 1. Standard nonlinear least-squares fits were obtained for at least four stretches of different

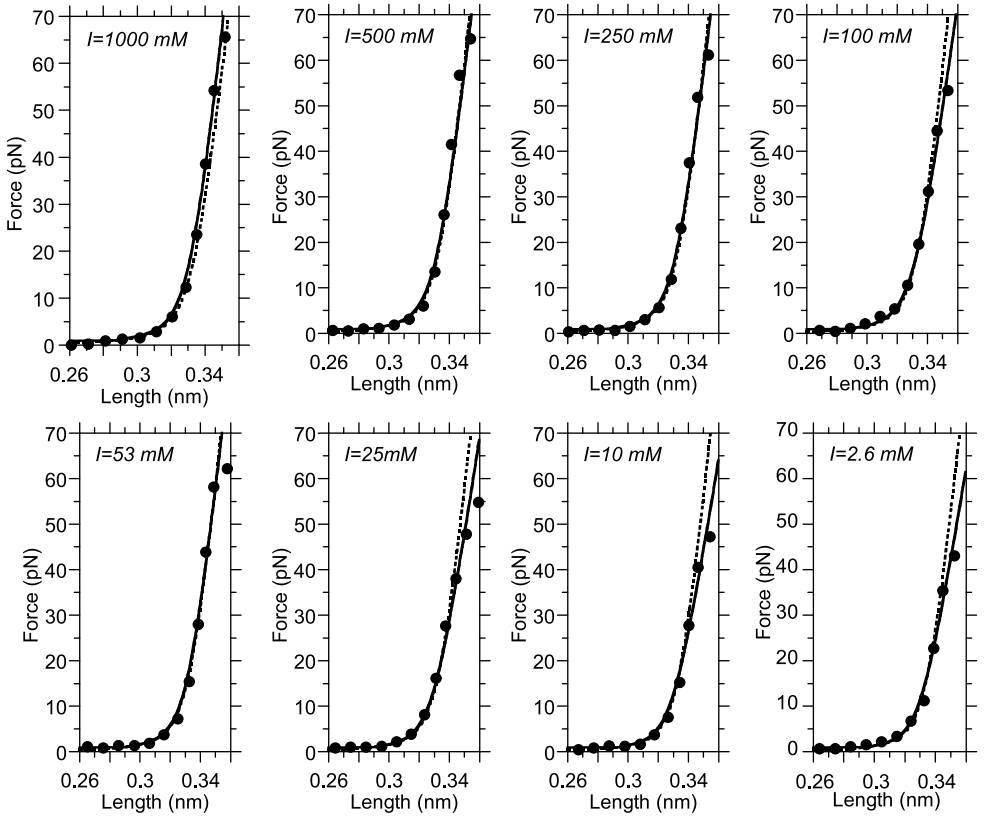

FIGURE 2 Partial DNA stretching curves at [Na^+] ranging from 1000 to 2.57 mM. The data (●) are representative measurements from a single stretch of a DNA molecule. The solid lines are calculated from Eq. 1 using the values obtained from fitting P_{ds} and K_{ds} independently (three-parameter fit). The dashed lines are the results of a two-parameter fit to the data (see text). The error in force measurement for these curves is ± 0.5 pN. For both fitting procedures, only the data points between 1 and 40 pN were used in the fit.

TABLE 1 DNA elasticity parameters and measured overstretching force

	Three-Parameter Fit		Two-Parameter Fit		
[Na+]	P_{ds} (nm)	K_{ds} (pN)	P_{ds} (nm)	K_{ds} (pN)	F_{os} (pN)
1000	46 ± 2	1256 ± 217	46 ± 2	1256 ± 217	68.0 ± 0.9
500	47 ± 2	1049 ± 226	44 ± 2	1295 ± 217	67.3 ± 1.2
250	46 ± 1	1038 ± 69	45 ± 2	1278 ± 217	65.5 ± 0.8
100	48 ± 2	884 ± 116	47 ± 2	1266 ± 217	62.6 ± 0.7
53.5	52 ± 1	1078 ± 64	46 ± 2	1260 ± 217	61.0 ± 0.7
25	58 ± 3	790 ± 104	47 ± 2	1255 ± 217	58.8 ± 1.2
10	67 ± 4	741 ± 147	56 ± 4	1250 ± 217	55.3 ± 1.2
2.6	68 ± 2	741 ± 56	59 ± 2	1243 ± 217	51.5 ± 1.2

Data shown are mean ± SE, $n \geq 3$.

P_{ds} and K_{ds} are the persistence length and stretch modulus from fits to the force–extension curves at low force ($F < 40$ pN) using Eq. 1. In the three-parameter fit, P_{ds} and K_{ds} are allowed to vary independently. In the two-parameter fit, the effective charge density of dsDNA is used to determine K_{ds} from Eq. 3, and P_{ds} is fit to the data with this constraint. The additional parameter in Eq. 1, b_{ds}^{max}, did not vary systematically and was always 0.34 ± 0.01 in these fits. F_{os} is the overstretching force measured at the midpoint of the transition shown in Fig. 5.

DNA molecules using Eq. 1 over the force range 1 pN $<$ $F < 40$ pN. Each fit gave three parameters, b_{ds}^{max}, P_{ds}, and K_{ds}, and an error in the fit of each parameter. However, allowing b_{ds}^{max} to vary independently in the fitting routine resulted in high error values in the determination of P_{ds}, and K_{ds}. In addition, the value of b_{ds}^{max} can vary between different molecules depending on the details of the attachment. Therefore, for the fits obtained here, b_{ds}^{max} was varied manually to minimize the relative error in the fits of P_{ds} and K_{ds}. Standard methods were then used to obtain the weighted mean and average variance of the resulting parameters from several curves (Bevington and Robinson 1992), which are reported in Table 1. The force–extension curves obtained from the values reported in Table 1 are shown as solid lines in Fig. 2, along with the data from one representative stretch (●).

The low salt data (<250 mM) in Fig. 2 were obtained from the initial stretch of the DNA molecule to reduce the possibility of inadvertently measuring the properties of ssDNA. In low salt, hysteresis is always observed upon relaxation of single DNA molecules. Most of the time, the original stretching curve is obtained upon subsequent stretches, with the hysteresis reappearing upon relaxation. However, we found that some DNA molecules display double-stranded character on the initial stretch, and partially ssDNA character on subsequent stretches (Fig. 3). Conversion to ssDNA upon stretching was more frequent at low salt concentration. We also note in Fig. 3 that it is not necessary to stretch DNA all the way through the overstretching transition to obtain partially ssDNA. This indicates that DNA denaturation occurs during the transition.

DNA overstretching transition

Full stretching curves obtained at 10, 100, and 1000 mM salt concentration are shown in Fig. 4. When the DNA is extended beyond its contour length, the force plateaus until the DNA is pulled to ~1.7 times its B-form contour length. According to the theory of Rouzina and Bloomfield (2001a), the plateau in Fig. 4 signifies a transition from the double-stranded state, represented by the solid line on the left, to the single-stranded state, represented by the solid line on the right. The force rises again after the plateau with a slope that depends on pulling rate, until ~140 pN, where the force–extension curve of dsDNA then matches ssDNA (Hegner et al. 1999; Clausen-Schaumann et l. 2000). This final portion of the dsDNA curve represents nonequilibrium melting because relatively few bonds remain between the strands, and the rupture force depends on the pulling rate. (Evans and Ritchie 1997).

The extensible freely jointed chain (FJC) model can be used to fit the force–extension curve of ssDNA (Smith et al. 1992),

$$b_{ss}(F) = b_{ss}^{max}\left(\coth(2\tilde{F}) - \frac{1}{2\tilde{F}}\right) \cdot \left(1 + \frac{F}{K_{ss}}\right), \quad (2)$$

where $\tilde{F} = FP_{ss}/k_BT$ is the reduced force, b_{ss}^{max} is the contour length per base in ssDNA, and P_{ss} is the persistence length of ssDNA. Experimental measurements of ssDNA stretching at pH 8 and 150 mM [Na^+] give FJC fit values of P_{ss} = 0.75 nm, b_{ss}^{max} = 0.56 nm, and K_{ss} = 800 pN (Smith et al. 1996).

The overstretching portions of the force–extension curves as a function of salt are shown in Fig. 5. The overstretching force decreases as [Na^+] is decreased, as expected for a force-induced melting transition. Many of the molecules broke while being extended, particularly at low [Na^+], which may be due to single-strand nicks in the DNA strand attached to the beads (despite the treatment with ligase) or a decrease in the biotin–streptavidin bond strength at low [Na^+].

To analyze the stretching behavior quantitatively, we have drawn a straight line through the linear region of each transition curve in Fig. 5, and extended it to the intersection with the wormlike chain curves for dsDNA and freely jointed chain curves for ssDNA. We define the overstretching force as the force required to stretch a DNA molecule halfway through the overstretching transition, or half the length between the dsDNA curve and the ssDNA curve shown in Fig. 4. The position along the fit line corresponding to the transition midpoint was evaluated and the force at this point, denoted F_{os}, is shown in Fig. 6 and presented in Table 1 as a function of [Na^+]. The width of the overstretching transition remained constant at ~4 pN.

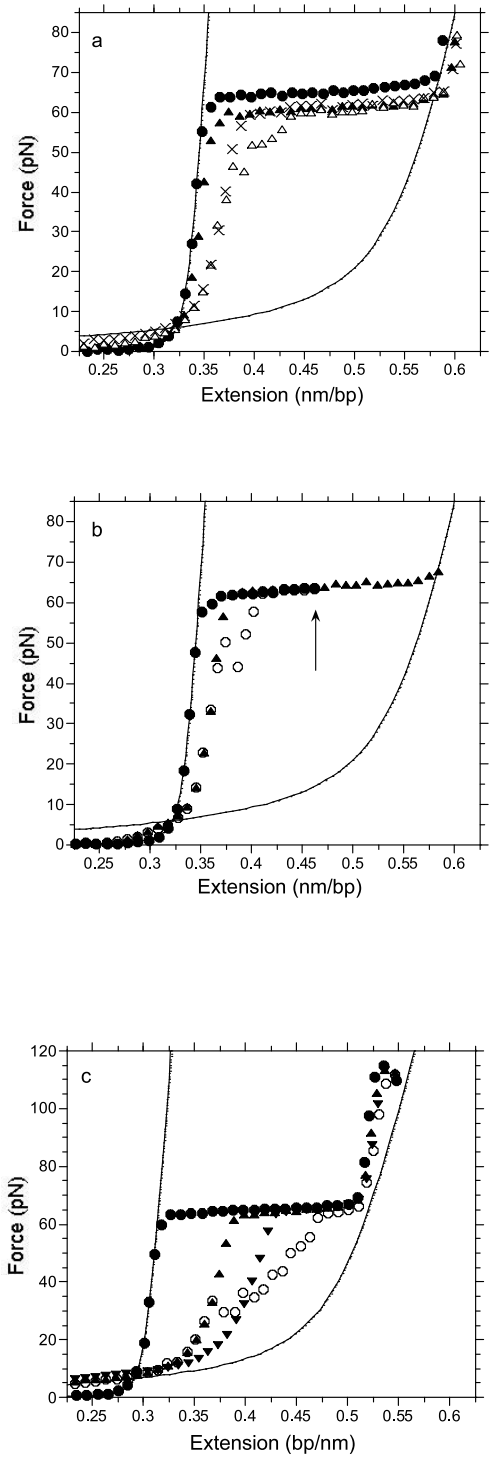

FIGURE 3 Stretching dsDNA may produce partially ssDNA. (*A*) A single molecule of dsDNA that has been tethered and stretched twice in 250 mM buffer (●) and three times in 100 mM buffer (data not shown), converts to partially ssDNA during the second stretch in 53 mM buffer (▲). The 53-mM relaxation curve (△) and subsequent stretch (×) overlap and display partial ssDNA character. Lines representing the WLC model (Eq. 1) with $P_{ds} = 50$ nm and $K_{ds} = 1200$ pN, and the FJC model with $b_{ss}^{max} = 0.56$ nm, $P_{ss} = 0.75$, and $K_{ss} = 800$ pN (Smith *et al.* 1996) are also shown. (*B*) A single dsDNA molecule that has been tethered and stretched to 0.46 nm/bp (*arrow*) in 250 mM buffer (●), displays partial ssDNA character during the relaxation curve (○) and subsequent stretch (▲). (*C*) Multiple stretches to high extensions produce partially ssDNA. A dsDNA molecule that has been tethered in 250 mM buffer and stretched to near the maximum force achievable with this instrument (●) displays large hysteresis and partial ssDNA character during relaxation (○). Second (▲) and third (▼) stretches increase ssDNA character, but additional stretching to high force failed to produce fully ssDNA.

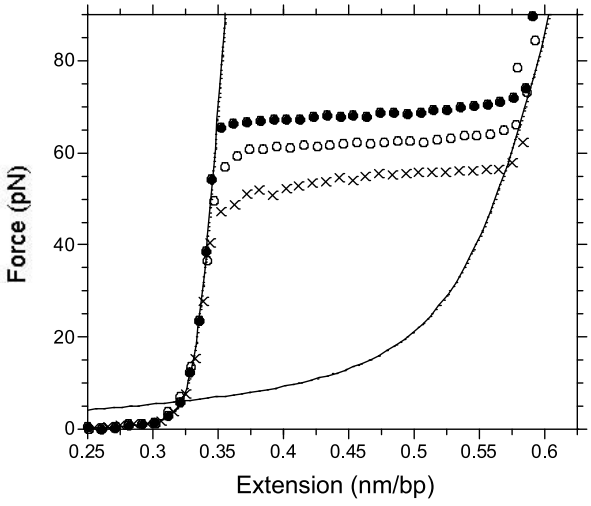

FIGURE 4 Room temperature force–extension (per base pair) curves for a single dsDNA molecule in 1000 mM (●), 100 mM (○), and 10 mM (×) [Na^+] buffer at pH 7.5. The solid lines represent the extensible WLC (*left*) and FJC (*right*) as described in Fig. 2. The data are interpreted as a transition between dsDNA (*left*) and ssDNA (*right*).

DISCUSSION

DNA elasticity

According to classical elasticity theory, the persistence length and stretch modulus of a thin rod made of homogeneous, elastic continuum should be proportional to each other (Landau and Lifshitz 1986). However, the data of Table 1 indicate that, as salt concentration is decreased, the persistence length of DNA, often naively regarded as the bending stiffness divided by k_BT, increases while the stretch modulus decreases. This is most likely due to the electrostatic repulsion between the phosphates on the negatively charged backbone on DNA. As the salt concentration is lowered, the screening of the electrostatic interactions decreases, thus making it easier to stretch the DNA while simultaneously making the molecule more rigid (Podgornik et al. 2000).

The effect of these electrostatic interactions has been calculated (Podgornik et al. 2000). The [Na^+] dependence of the elastic stretch modulus is given by

$$K_{ds}([Na^+]) = K_0 - \delta K$$

$$= K_0 - \frac{k_BT \cdot l_B}{a^2} g(\kappa b), \qquad (3)$$

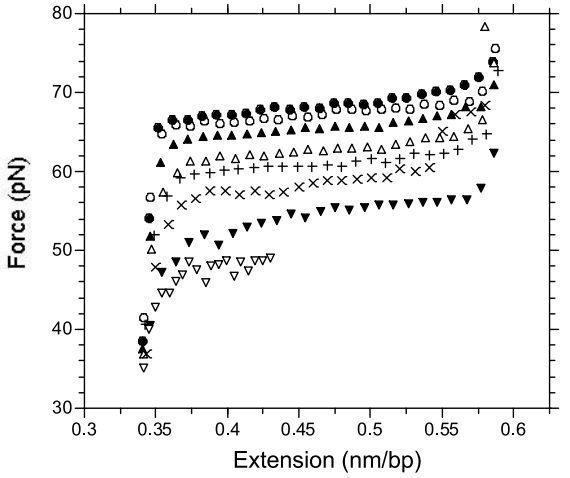

FIGURE 5 Overstretching portions of the DNA force–extension curves as a function of [Na^+]. The overstretching force decreases with salt concentration. The data were obtained by stretching single DNA molecules in solutions with [Na^+] of 1000 mM (●), 500 mM (○), 250 mM (▲), 100 mM (△), 50 mM (+), 25 mM (×), 10 mM (▼), and 2.6 mM (▽).

where the $g(x)$ function is approximated as

$$g(x) = e^{-x} - Ei(x)$$
$$\approx e^{-x} - 0.577 - \ln(x) - x - \frac{x^2}{4} - \frac{x^3}{18} - \frac{x^4}{96},$$

and where K_0 is the limiting high salt (nonelectrostatic) value, δK is the electrostatic contribution, $l_B = e^2/\varepsilon k_B T$ is the Bjerrum length, $\kappa = \sqrt{8\pi[Na^+]l_B}$ is the Debye screening parameter, $Ei(x)$ is the exponential integral function, a is the effective length per charge of DNA after counterion condensation, and b is the radius of the DNA molecule. The results are not very sensitive to the value of b, so this parameter is fixed at 1 nm in our calculations. Eq. 3 can be obtained by substituting Eq. 29 into Eq. 28 of Podgornik et al. (2000) and solving the resulting quadratic equation for δK ($\delta\lambda$ in their notation), noting that there is a sign error in Eq. 28, which should contain the expression $Ei(\kappa b)$ rather than $Ei(-\kappa b)$. It is also necessary to assume that $K_{ds} \gg F$.

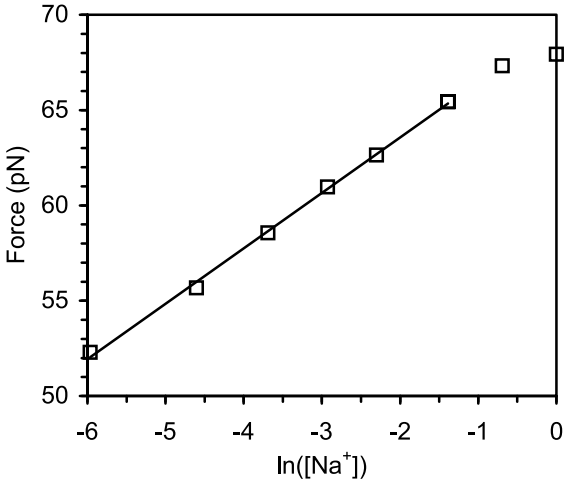

FIGURE 6 Measured overstretching force as a function Na^+ concentration. The error in force measurement is given in Table 1. The solid line is a linear fit to the data, which yields a value of v = 0.49 from Eq. 7.

The [Na^+] dependence of the persistence length is given by the expression

$$P_{ds} = P_0 + \frac{\alpha}{32\pi[Na^+]a^2}$$
$$\approx P_0 + \frac{0.324}{I} \cdot \left(\frac{l_B}{a}\right)^2, \quad (4)$$

where $\alpha = (1 - \delta K/K_0)^3$, which represents a correction to the standard Odijk–Skolnick–Fixman formula for the [Na^+] dependence of the persistence length (Odijk 1977; Skolnick and Fixman 1977) due to the extensibility of the polymer. For dsDNA, this correction appears to be negligible. In the second part of Eq. 4, the salt concentration I should be expressed in molar units and P_0 in Å. Also, P_0 is the nonelectrostatic persistence length measured at high salt concentrations, and a is the effective length per charge of DNA. Eqs. 3 and 4 can then be fit to our measurements by adjusting the effective charge density of DNA. The results are shown in Fig. 7 *A*, along with the data from Baumann et al. (1997). The results obtained here are also presented in Table 1.

Nonlinear least squares fitting of our data yields a = 5.5 ± 0.9 Å when fitting the persistence length and a = 2.6 ± 0.2 Å when fitting the stretch modulus. Similarly, the data of Baumann et al. (1997) yields a = 4.5 ± 0.2 Å when fitting the persistence length and a = 1.7 ± 0.2 Å when fitting the stretch modulus. However, the effective length per charge of DNA should be the same for both calculations. Therefore, instead of fitting our data to Eq. 1 and allowing P_{ds} and K_{ds} to vary independently, we would like to fit the data to the single variable parameter a.

To do this, we fix K_0 and P_0 to the values measured at 1 M [Na^+] and use Eqs. 3 and 4 to calculate K_{ds}([Na^+]). We then fix K_{ds}([Na^+]) at the calculated value for each salt concentration and fit Eq. 1 to the data to determine P_{ds}([Na^+]). The value of a is then determined by fitting Eq. 4 to the data for P_{ds}([Na^+]). K_{ds}([Na^+]) is then recalculated and the fitting procedure repeated. The resulting values of P_{ds}([Na^+]) and K_{ds}([Na^+]) are shown in Table 1 and are also shown in Fig. 7 *B* (*closed* and *open triangles*, respectively). From our fit of P_{ds}([Na^+]) (derived from the two parameter fit of force-extension data) to Eq. 4, we find that α = 6.7 ± 0.7 Å. This value for the linear charge density is consistent with polyelectrolyte theory, which predicts that $\alpha = l_B$ = 7.2 Å in water at room temperature. The solid and dashed lines in Fig. 7 *B* are the theoretical values for P_{ds}([Na^+]) and K_{ds}([Na^+]) from Eqs. 3 and 4 using this value of a. The symbols presented for

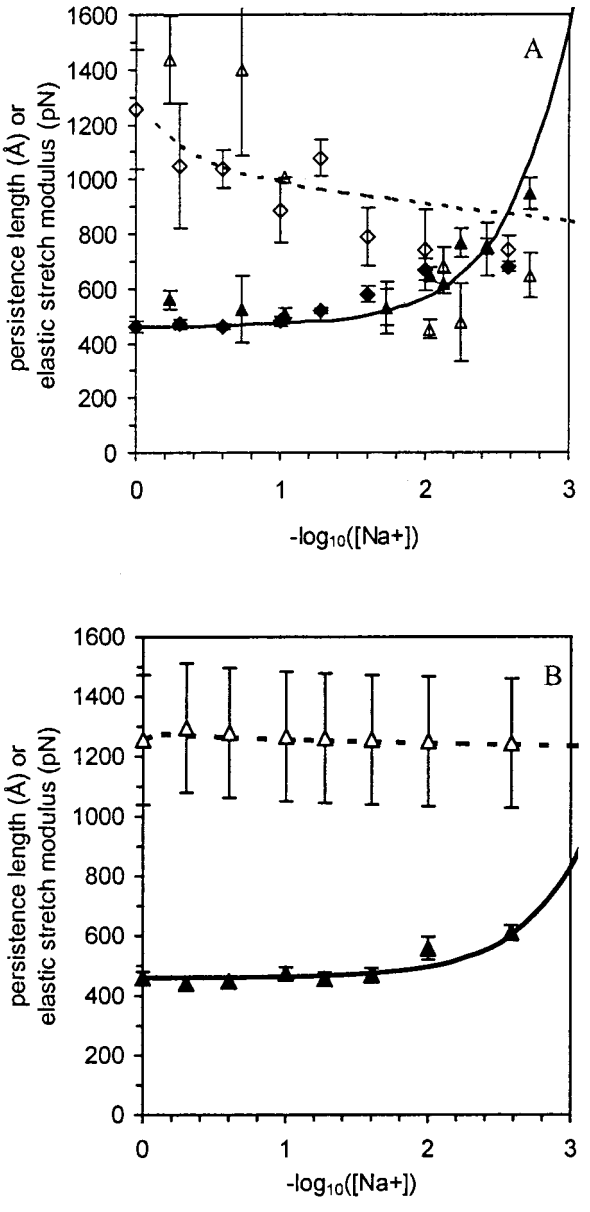

FIGURE 7 (*A*) Values of P_{ds} (◆) and K_{ds} (◇) obtained from fits to DNA stretching curves in which the parameters are allowed to vary independently (three-parameter fit). Fits of P_{ds} (*solid line*) and K_{ds} (*dashed line*) to the theory of Podgornik et al. (2000) are also shown, as well as the results from Baumann et al. (1997) for P_{ds} (▲) and K_{ds} (△). (*B*) Values of P_{ds} (▲) obtained from a two-parameter fit in which K_{ds} (*dashed line*) is calculated from Eq. 4 and the stretching curve is fit assuming a fixed value of K_{ds} (△). The theoretical curve for P_{ds} (*solid line*) calculated from Eq. 4 with a = 0.67 nm is also shown.

$K_{ds}([Na^+])$ in Fig. 7 *B* and the data in column 5 of Table 1 result from the same calculation as the dashed line, but they also show the error in determination of $K_{ds}([Na^+])$, which results from the error in K_0.

The actual fits to the stretching data obtained by using this procedure are shown in Fig. 2 as dashed lines for each salt concentration. The systematic deviations of the fits from the data in Fig. 2 at high forces and low salt represent DNA force-induced melting, which occurs at lower forces under these conditions. This may contribute to the stronger salt dependence of K in the 3-parameter fit. In other words, the effect of low salt on *f–x* curve at the extensions slightly beyond the B-DNA contour length could be attributed either to the beginning of the overstretching transition or to the softening of the elastic modulus of B-DNA. However, if only the part of the force-extension curve that is not affected by the overstretching transition is fit, the obtained values of $P_{ds}([Na^+])$, $K_{ds}([Na^+])$, and a are fully consistent with the predictions of polyelectrolyte theory. Although we have not applied our new analysis to the force–extension data presented in Baumann et al. (1997)), it is likely that similar results would be obtained, given that we obtain similar results when allowing $P_{ds}([Na^+])$ and $K_{ds}([Na^+])$ to be fit independently.

We have shown that P_{ds} and K_{ds} cannot be uniquely determined by fitting them independently, so the results from such fits cannot be used to draw conclusions about theories describing their salt dependence, such as the theory of Podgornik et al (2000)). We have demonstrated for this theory that the predicted dependence of $P_{ds}([Na^+])$ and $K_{ds}([Na^+])$ is consistent with our measured stretching curves. By assuming $K_{ds}([Na^+])$ from this theory, we were able to show that the resulting fits to our data yield reasonable values of $P_{ds}([Na^+])$ and provide an accurate determination of the linear charge density of DNA that is consistent with polyelectrolyte theory.

DNA overstretching

To better understand the changes that take place during DNA overstretching, we can use polyelectrolyte theory to predict the $[Na^+]$ dependence of the stability of DNA based only on changes in the charge density of DNA during overstretching. The theory that we will use is valid only in low salt ($[Na^+] \ll$ 1 M), so we will compare it with our data at $[Na^+]$ of 100 mM or less. Under these conditions, the salt-dependent part of the helix-coil transition free energy is given by (Bond et al. 1994; Frank-Kamenetskii et al. 1987)

$$\Delta G_{el} = k_B T\left(\frac{1}{\xi_{ss}} - \frac{1}{\xi_{ds}}\right)\ln\left(\frac{[Na^+]}{[Na^+]_0}\right), \quad (5)$$

where ξ is the dimensionless linear charge density,

$$\xi = \frac{l_B}{h}, \quad (6)$$

where h is the length per unit charge and l_B the Bjerrum length. From these relations, we find that the variation of the

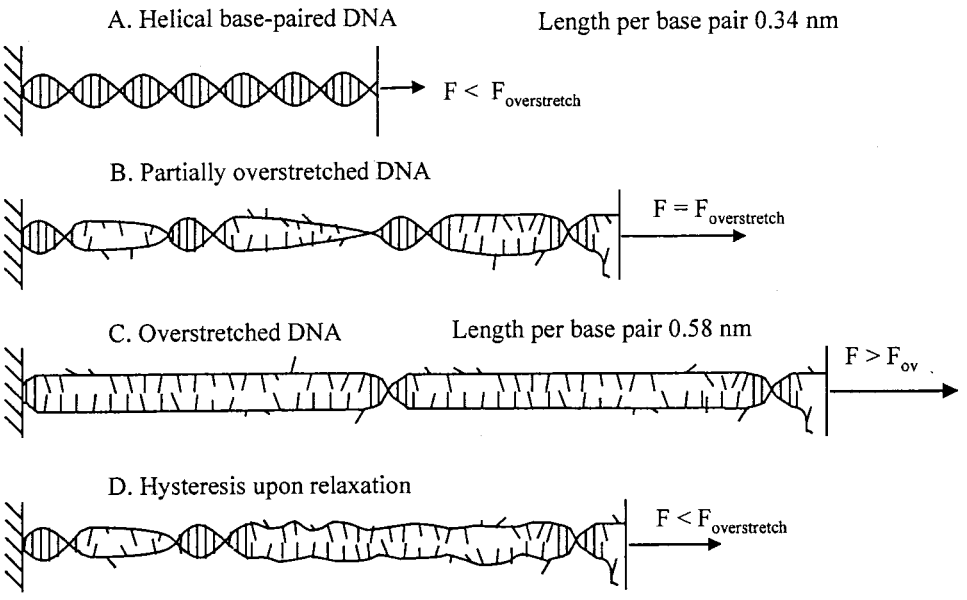

FIGURE 8 Schematic diagram of force-induced melting model. (*A*) When DNA is stretched at forces less than the overstretching force, denoted F_{os}, the bases remain paired and the helical form is maintained. (*B*) During the overstretching transitions, domains of melted DNA are separated by helical sections. (*C*) At the end of the transition, short, helical domain boundaries hold the largely melted strands together. (*D*) One predicted consequence of the model is that the separated base pairs may not bind immediately when the molecule is relaxed. Thus, when the molecule is relaxed to the same extension shown in (*B*), the observed force is less than F_{os}.

overstretching force with $[Na^+]$ is given by (Rouzina and Bloomfield 2001b)

$$\frac{\partial f_{os}}{\partial \ln([Na^+])} = \frac{k_B T}{l_B}\nu \tag{7}$$

where

$$\nu = \frac{h_{ss} - h_{ds}}{b_{ss} - b_{ds}} \tag{8}$$

is the ratio of the difference in length per unit charge and the change in length per base pair in the direction of the force when DNA is overstretched. If the distance between the DNA strands is less than the Debye screening length, $r_D = 1/\kappa$, then the two strands are equivalent to a single strand with twice the charge density, so $\nu = 0.5$. If the average distance between strands is greater than the Debye screening length, then $\nu = 1.7$. If one strand is stretched while the other is relaxed, then we have $\nu = 1.2$ (Rouzina and Bloomfield 2001b). Thus, fits of our data to Eq. 7 will allow us to determine the state of the two strands during the overstretching transition. A similar calculation was originally presented in Stigter (1998). The solid line in Fig. 6 is a linear fit to the measured overstretching force as a function of $\ln([Na^+])$. Evaluating the slope of this line gives a value of $\nu = 0.49$ from Eq. 8. Thus, our data support the idea that both DNA strands are stretched and remain very close to each other during the overstretching transition.

In our measurements, the dependence of F_{os} on $[Na^+]$ is somewhat weaker than that observed by Baumann et al. (1997) (see panel A of Fig. 2 in Baumann et al.). It is important to note here that our F_{os} values were obtained on the DNA stretching curves that exhibited a complete or almost complete overstretching transition, whereas the stretches from DNA molecules that broke at some point during the overstretching transition were discarded. By doing this, we, in fact, selected for the DNA molecules containing the minimum number of single-stranded nicks. In Baumann et al. (1997) this selection was not performed. As was shown in (Rouzina and Bloomfield 2001b) the slope of F_{os} versus $\ln[Na^+]$ can depend on the number of nicks in the molecule, because it determines the proportion of the DNA regions with just one or both strands under tension. Thus the differences in the dependence of F_{os} on $[Na^+]$ in these two experiments are within the expected range, and are fully consistent with the melting nature of the overstretching transition.

A model for the structure of overstretched DNA based on all available data regarding the dependence of the transition on solution conditions is shown in Fig. 8. When the DNA is stretched to extensions less than the contour length, the molecule consists entirely of dsDNA (Fig. 8 *A*). Based on the pH and temperature dependence of F_{os} we have shown that the base pairs holding the two DNA strands together must break (Williams et al. 2001a,b). Because of the one-dimensional nature of DNA melting and its sequence het-

erogeneity, it is favorable to create melted domains of DNA that are separated by regions of unmelted DNA. This behavior is well known from thermal DNA melting studies, where it has been determined that the average size of a melted domain at the midpoint of a melting transition is ~100 bp (Cantor and Schimmel 1980). A model for how this might occur in overstretched DNA is shown in Fig. 8 *B*. It has been shown (Hegner et al. 1999) that the DNA strands do not completely separate until the molecule is stretched to forces of 150 pN or greater. Thus, short base-paired sections must remain at the end of the transition (Fig. 8 *C*). Removal of these last base pairs represents an irreversible process, so forces greater than F_{os} are required to completely separate the DNA strands. This model is consistent with early DNA melting studies that showed that DNA strand separation did not occur until the DNA molecules were heated to temperatures much greater than the melting temperature (Geiduschek 1962). This model also explains the hysteresis observed in our DNA stretching studies (Fig. 8 *D*). As the DNA is relaxed, the base pairs must reanneal in the correct sequence. If the DNA is relaxed quickly, some of the sequences are not in the helical form, so a lower force is required to stretch the molecule. The effect is more pronounced in low salt because electrostatic repulsion prevents the strands from properly reannealing. In high salt, the screening due to the high concentration of counterions allows quick reannealing to occur.

CONCLUSIONS

In this work, we have measured DNA elasticity and the DNA overstretching transition as a function of salt concentration. We have shown that polyelectrolyte theory adequately describes the salt dependence of both the dsDNA persistence length and elastic stretch modulus. Our data thus help to explain the discrepancy between the predictions of simple elasticity theory (Landau and Lifshitz 1986) and the observed changes in DNA stretching properties with $[Na^+]$.

We have also shown that destabilizing the DNA double helix by decreasing the solution $[Na^+]$ causes a decrease in the overstretching force, as is expected for a force-induced melting transition. Our data are consistent with the interpretation of the overstretching transition of dsDNA as a force-induced melting transition. In addition to the agreement between the prediction of the $[Na^+]$ dependence of the overstretching transition and the measured data, we also see significant hysteresis at low $[Na^+]$, when the DNA double helix is destabilized. At low $[Na^+]$, a DNA molecule that was stretched only partially through the overstretching transition displayed single-stranded DNA character, indicating that a section of one strand of the DNA molecule had melted during the overstretching transition. This indicates that DNA melting occurs during the overstretching transition, rather than at the end of the transition.

By fitting the $[Na^+]$ dependence of DNA overstretching to polyelectrolyte theory, we have also shown that the two DNA strands from a single molecule remain stretched and close together during the transition. Although this result cannot be used to distinguish between the models of S-DNA and the force-induced melting model of DNA overstretching, it is consistent with the force-induced melting model (Rouzina and Bloomfield 2001a), whereas the observed hysteresis at low salt supports force-induced melting. In the force-induced melting model, the strands are held close together by a small number of base pairs that represent boundaries between melted domains. These domain boundaries are not removed until after the end of the transition, so the strands remain close together, even as most of the base pairs separate during the transition.

We thank Prof. Matthew Tirrell and the University of Minnesota Center for Interfacial Engineering for funding and assistance in starting the optical tweezers project. We are grateful to Drs. Steve Smith and Christoph Baumann for help with protocols and instrument-building advice, and to Dori Henderson for taking the time to make a number of glass micropipettes for use in our experiments. We also thank the anonymous reviewers for helping us to clarify some points in the manuscript.

Funding for this project was provided by grants from National Institutes of Health (GM28093) and National Science Foundation (MCB9728165).

REFERENCES

Ahsan, A., J. Rudnick, and R. Bruinsma. 1998. Elasticity theory of the B-DNA to S-DNA transition. *Biophys. J.* 74:132–137.

Allemand, J. F., D. Bensiomon, R. Lavery, and V. Croquette. 1998. Stretched and overwound DNA forms a Pauling-like structure with exposed bases. *Proc. Natl. Acad. Sci. USA.* 95:14152–14157.

Baumann, C. G., S. B. Smith, V. A. Bloomfield, and C. Bustamante. 1997. Ionic effects on the elasticity of single DNA molecules. *Proc. Natl. Acad. Sci. U.S.A.* 94:6185–6190.

Bennink M. L., O. D. Schaerer, R. Kanaar, K. Sakata-Sogawa, J. M. Schins, J. S. Kanger, B. G. de Grooth, and J. Greve. 1999. Single-molecule manipulation of double-stranded DNA using optical tweezers: interaction studies of DNA with RecA and YOYO-1. *Cytometry*. 36: 200–208.

Bevington, P. R., and D. K. Robinson. 1992. Data Reduction and Error Analysis for the Physical Sciences. McGraw-Hill, Boston, MA.

Bond J. P., and C. F., Anderson. M. T. Record. 1994. Conformational transitions of duplex and triplex nucleic acid helices—thermodynamic analysis of effects of salt concentration on stability using preferential interaction coefficients. *Biophys. J.* 67:825–836.

Bouchiat C., M. D. Wang, J. F. Allemand, T. Strick, S. M. Block, and V. Croquette. 1999. Estimating the persistence length of a worm-like chain molecule from force–extension measurements. *Biophys. J.* 76:409–413.

Bustamante, C., J. Marko, E. Siggia, and S. Smith. 1994. Entropic elasticity of lambda-phage DNA. *Science.* 265:1599–1600.

Cantor, C. R., and P. R. Schimmel. 1980. Biophysical Chemistry. W. H. Freeman and Company, New York.

Cizeau P., and J. L. Viovy. 1997. Modeling extreme extension of DNA. *Biopolymers.* 42:383–385.

Clausen-Schaumann H., M. Rief, C. Tolksdorf, and H. E. Gaub. 2000. Mechanical stability of single DNA molecules. *Biophys. J.* 78: 1997–2007.

Cluzel P., A. Lebrun, C. Heller, R. Lavery, J. L. Viovy, D. Chatenay, and F. Caron. 1996. DNA: an extensible molecule. *Science.* 271:792–794.

Evans E., and K. Ritchie. 1997. Dynamic strength of molecular adhesion bonds. *Biophys. J.* 72:1541–1555.

Frank-Kamenetskii M. D., V. V. Anshelevich, and A. V. Lukashin. 1987. Polyelectrolyte model of DNA. Soviet Physics—Uspekhi 151:595–618. (Translation).

Geiduschek, E. P. 1962. On the factors controlling the reversibility of DNA denaturation. *J. Mol. Biol.* 4:467–487.

Grosberg A. Y., and A. R. Khokhlov. 1994. Statistical Physics of Macromolecules. American Institute of Physics, New York.

Haijun Z., Z. Yang, and O.-Y. Zhong-can. 1999. Bending and base-stacking interactions in double-stranded DNA. *Phys. Rev. Lett.* 82: 4560–4563.

Hegner M., S. B. Smith, and C. Bustamante. 1999. Polymerization and mechanical properties of single RecA-DNA filaments. *Proc. Nat. Acad. Sci. U.S.A.* 96:10109–10114.

Konrad, M. W., and J. I. Bolonick. 1996. Molecular dynamics simulation of DNA stretching is consistent with the tension observed for extension and strand separation and predicts a novel ladder structure. *J. Am. Chem. Soc.* 118:10989–10994.

Kosikov, K. M., A. A. Gorin, V. B. Zhurkin, and W. K. Olson. 1999. DNA stretching and compression: large-scale simulations of double helical structures. *J. Mol. Biol.* 289:1301–1326. [Review]

Landau, L. D., and E. M. Lifshitz. 1986. Theory of Elasticity. Pergamon, Oxford. U.K.

Lebrun A, R. Lavery 1996. Modelling extreme stretching of DNA. *Nucleic Acids Res.* 24:2260–2267.

Leger, J. F., G. Romano, A. Sarkar, J. Robert, L. Bourdieu, D. Chatenay, and J. F. Marko. 1999. Structural transitions of a twisted and stretched DNA molecule. *Phys. Rev. Lett.* 83:1066–1069.

Manning, G. S. 1978. The molecular theory of polyelectrolyte solutions with applications to the electrostatic properties of polynucleotides. *Q. Rev. Biophys.* 11:179–246.

Marko, J. F. 1998. DNA under high tension: overstretching, undertwisting, and relaxation dynamics. *Phys. Rev. E.* 57:2134–2149.

Marko, J. F., and E. D. Siggia. 1995. Stretching DNA. *Macromolecules.* 28:8759–8770.

Mehta, A, J. Finer, and J. Spudich. 1998. Reflections of a lucid dreamer: optical trap design considerations. *Methods Cell Biol* 55:47–69.

Odijk, T. 1977. Polyelectrolytes near the rod limit. *J. Polym. Sci. Polym. Phys. Ed.* 15:477–483.

Odijk, T. 1995. Stiff chains and filaments under tension. *Macromolecules.* 28:7016–7018.

Podgornik, R., P. L. Hansen, and V. A. Parsegian. 2000. Elastic moduli renormalization in self-interacting stretchable polyelectrolytes. *J. Chem. Phys.* 113:9343–9350.

Rief M., H. Clausen-Schaumann, and H. E. Gaub. 1999. Sequence-dependent mechanics of single DNA molecules. *Nature Struct. Biol.* 6:346–349.

Rouzina, I., and V. A. Bloomfield. 2001a. Force-induced melting of the DNA double helix 1. Thermodynamic analysis. *Biophys. J.* 80:882–893.

Rouzina, I., and V. A. Bloomfield. 2001b. Force-induced melting of the DNA double helix 2. Effect of solution conditions. *Biophys. J.* 80: 894–900.

Skolnick, J., and M. Fixman. 1977. Electrostatic persistence length of a wormlike polyelectrolyte. Macromolecules 10:944–948.

Smith S. B., Y. J. Cui, and C. Bustamante. 1996. Overstretching B-DNA: the elastic response of individual double-stranded and single-stranded DNA molecules. *Science.* 271:795–799.

Smith, S. B., L. Finzi, and C. Bustamante. 1992. Direct mechanical measurements of the elasticity of single DNA molecules by using magnetic beads. *Science.* 258:1122–1126.

Stigter, D. 1998. An electrostatic model of B-DNA for its stability against unwinding. *Biophys. Chem.* 75:229–233.

Wenner, J. R., and V. A. Bloomfield. 1999. Buffer effects on *Eco*RV kinetics as measured by fluorescent staining and digital imaging of plasmid cleavage. *Anal. Biochem.* 268:201–212.

Williams, M. C., J. R. Wenner, I. Rouzina, and V. A. Bloomfield. 2001a. The effect of pH on the overstretching transition of dsDNA: evidence of force-induced DNA melting. *Biophys. J.* 80:874–882.

Williams, M. C., J. R. Wenner, I. Rouzina, and V. A. Bloomfield. 2001b. Entropy and heat capacity of DNA melting from temperature dependence of single molecule stretching. *Biophys. J.* 80:1932–1939.